

Improved criteria of detecting multipartite entanglement structure

Kai Wu and Zhihua Chen*

School of Science, Jimei University, Xiamen 361021, China

Zhen-Peng Xu†

School of Physics and Optoelectronics Engineering, Anhui University, Hefei 230601, China

Zhihao Ma‡

*School of Mathematical Sciences, MOE-LSC, Shanghai Jiao Tong University, Shanghai 200240, China
Shanghai Seres Information Technology Co., Ltd, Shanghai 200040, China and
Shenzhen Institute for Quantum Science and Engineering,
Southern University of Science and Technology, Shenzhen 518055, China*

Shao-Ming Fei§

*School of Mathematical Sciences, Capital Normal University, Beijing 100048, China and
Max Planck Institute for Mathematics in the Sciences, 04103 Leipzig, Germany*

Multipartite entanglement is one of the crucial resources in quantum information processing tasks such as quantum metrology, quantum computing and quantum communications. It is essential to verify not only the multipartite entanglement, but also the entanglement structure in both fundamental theories and the applications of quantum information technologies. However, it is proved to be challenging to detect the entanglement structures, including entanglement depth, entanglement intactness and entanglement stretchability, especially for general states and large-scale quantum systems. By using the partitions of the tensor product space we propose a systematic method to construct powerful entanglement witnesses which identify better the multipartite entanglement structures. Besides, an efficient algorithm using semi-definite programming and a gradient descent algorithm are designed to detect entanglement structure from the inner polytope of the convex set containing all the states with the same entanglement structure. We demonstrate by detailed examples that our criteria perform better than other known ones. Our results may be applied to many quantum information processing tasks.

I. INTRODUCTION

Multipartite quantum entanglement is crucial in quantum communication and information processing tasks including quantum computing, quantum cryptography and quantum teleportation [1]. Very different from the bipartite case, multipartite quantum entanglement has a rich structure. Two important concepts have been introduced to characterize such multipartite entanglement structure, i.e., the entanglement producibility and entanglement partitionability [2, 3]. Intuitively for pure states, the partitionability refers to the number of subsystems separable from each other in the multipartite system, while the entanglement producibility, refers to the size of the largest entangled subsystem. Recently, the entanglement stretchability has been coined [4], which stands for the difference between the entanglement producibility and entanglement partitionability.

Quantum entanglement structure has many applications, e.g., in spin chains and quantum metrology [3, 5–

7]. However, as the number of subsystems grows, verifying the entanglement structure becomes a hard problem [2, 3]. Though one can detect theoretically the entanglement structure via state tomography, it becomes infeasible in practice due to the exponential growth of the dimensions of the underlying Hilbert space. Significant efforts have been devoted in this direction to develop feasible techniques, such as the utilization of more convenient inequalities given by spin-squeezing and the entries of density matrices, local uncertainty relations, Wigner-Yanase skew information, Fisher information and machine learning[1, 6, 8–31]. Gradually, entanglement structure has also been detected experimentally [32–39] for special cases, like for Dicke states [33].

Recently, a systematic approach based on Young diagrams and the partitions of the tensor product space has been proposed to classify the entanglement structures[4, 40]. Based on these works, we propose a systematic method to construct linear criteria to verify the quantum entanglement structures in this paper, where the number of measurements needed grows polynomially with the system size in experiments.

On the other hand, an algorithm based on the adaptive polytope approximation has been proposed to certify quantum separability of bipartite and multipartite quantum systems [41], each iteration is a semidefinite pro-

* chenzhihua77@sina.com

† zhen-peng.xu@ahu.edu.cn

‡ mazhihao@sjtu.edu.cn

§ feishm@cnu.edu.cn

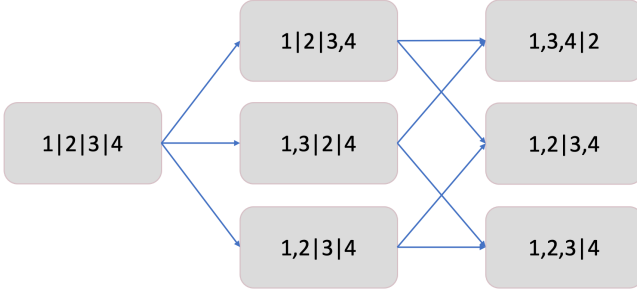


FIG. 1. Seven partitions of $\{1, 2, 3, 4\}$ are $\gamma_1 = 1|2|3|4$, $\gamma_2 = 1|2|3, 4$, $\gamma_3 = 1, 3|2|4$, $\gamma_4 = 1, 2|3|4$, $\gamma_5 = 1, 3, 4|2$, $\gamma_6 = 1, 2|3, 4$ and $\gamma_7 = 1, 2, 3|4$. The arrows in the diagram denote the refinement relationship, denoted by \preceq . For the partition set Γ consists of all seven partitions, $\Gamma^{\max} = \{\gamma_5, \gamma_6, \gamma_7\}$.

gramming (SDP). This algorithm updates each polytope in every iteration to ultimately achieve a satisfactory result, and depends on well-chosen initial polytopes so as to obtain a good enough result. Inspired by this algorithm, we proposed a new algorithm by employing the gradient descent method, which does not depend very much on the initial polytopes in obtaining a good enough result.

II. PRELIMINARY

A partition of a set is to classify each element into one and only one subset. For two partitions γ and ξ , we say γ is a refinement of ξ , denoted as $\gamma \preceq \xi$, if any subset in γ in a subset of the one in ξ . For a given pure state $|\psi\rangle$ in the form that $|\psi\rangle = \bigotimes_i |\psi_{X_i}\rangle$ where $\{X_i\}$ is a partition of the set of all parties, its entanglement structure can be represented by this partition. If an entanglement structure is representable by a partition γ and γ is a refinement of ξ , then it is also representable by the partition ξ .

Denote $|S|$ the size of the set S . For a given pure state $|\psi\rangle = \bigotimes_i |\psi_{X_i}\rangle$ and $\max |X_i| \leq k$, where $\{X_i\}$ is a partition of the set of all parties, $|\psi\rangle$ is said to be

1. k -producible, if $\max |X_i| \leq k$;
2. k -partitionable, if $|\{X_i\}| \leq k$;
3. k -stretchable, if $\max |X_i| - |\{X_i\}| \leq k$.

A mixed state ρ is called k -producible if it can be decomposed as a convex combination of k -producible pure states. Similarly, the definition of k -partitionable, or k -stretchable can be extended to mixed states.

Given a collection Γ of partitions, the set of maximal elements under the partial order of refinement \preceq is de-

noted Γ^{\max} . To continue, we introduce further notations:

$$\Gamma_{k\text{-part}} = \{\xi = \{X_i\} : |\{X_i\}| \leq k\}, \quad (1)$$

$$\Gamma_{k\text{-prod}} = \{\xi = \{X_i\} : \max |X_i| \leq k\}, \quad (2)$$

$$\Gamma_{k\text{-str}} = \{\xi = \{X_i\} : \max |X_i| - |\{X_i\}| \leq k\}. \quad (3)$$

Consequently, $\Gamma_{k\text{-prod}}^{\max}$, $\Gamma_{k\text{-part}}^{\max}$ and $\Gamma_{k\text{-str}}^{\max}$ can be defined. If the entanglement structure of a pure quantum state is representable by a partition within Γ , it is necessarily also representable by a partition within Γ^{\max} . An example is depicted in Fig. 1 with Γ to be the set of all the partitions of $\{1, 2, 3, 4\}$.

III. DETECTION OF ENTANGLEMENT STRUCTURE

Consider a direct product quantum state pairs $(|m\rangle, |n\rangle)$ with $|m\rangle = \bigotimes_{i=1}^N |m_i\rangle$, $|n\rangle = \bigotimes_{i=1}^N |n_i\rangle$, where $|m_i\rangle$ and $|n_i\rangle$ are the standard orthogonal basis of \mathcal{H}_i . We have the following result, which pertains to an inequality involving a off-diagonal element of a density matrix and two of its diagonal elements:

Proposition 1. For any pure state $|\psi\rangle = \bigotimes_{X_i \in \gamma} |\psi_{X_i}\rangle$ and $\forall X_i \in \gamma$, we have

$$|\langle m|\psi\rangle\langle\psi|n\rangle| \leq \frac{1}{2} [(\langle m_{\bar{X}_i}|\langle n_{X_i}||\psi\rangle\langle\psi|(|m_{\bar{X}_i}\rangle|n_{X_i}\rangle) + \langle m_{X_i}|\langle n_{\bar{X}_i}||\psi\rangle\langle\psi|(|m_{X_i}\rangle|n_{\bar{X}_i}\rangle)), \quad (4)$$

where \bar{X}_i stands for the complement set of the set X_i .

The proof is given in Appendix I. Violation of the inequality in Eq. (4) means that $|\psi\rangle \neq \bigotimes_{X_i \in \gamma} |\psi_{X_i}\rangle$.

Based on the inequality in Eq. (4), we continue to construct further criteria involving more off-diagonal elements.

A. Criteria based on the outer polytopes

Firstly, we take a 3-qubit pure quantum state $\rho = |\psi\rangle\langle\psi|$ to illustrate the whole procedure. Consider the set of off-diagonal elements $P = \{\rho_{2,3}, \rho_{2,5}, \rho_{3,5}\}$ and the partition $12|3$. If $|\psi\rangle = |\psi_{12}\rangle \otimes |\psi_3\rangle$, a sequence of inequalities can be derived from Proposition 1 as follows,

$$\begin{cases} |\rho_{2,3}| - \frac{1}{2}\rho_{1,1} - \frac{1}{2}\rho_{4,4} \leq 0, \\ |\rho_{2,5}| - \frac{1}{2}\rho_{1,1} - \frac{1}{2}\rho_{6,6} \leq 0, \\ |\rho_{3,5}| - \frac{1}{2}\rho_{3,3} - \frac{1}{2}\rho_{5,5} \leq 0. \end{cases} \quad (5)$$

Besides, any diagonal element of the state ρ is non-negative and the sum of the appeared diagonal elements

is no more than 1. These inequalities define a series of closed half-spaces, whose intersection results in a convex polytope [42], denoted by $\Theta_{12|3}(P)$. Thus, if $|\psi\rangle$ can be decomposed as the tensor product $|\psi_{12}\rangle \otimes |\psi_3\rangle$, we must have the corresponding elements of the density operator $\rho = |\psi\rangle\langle\psi|$ to be in the polytope $\Theta_{12|3}(P)$. Consequently, any mixed state of the same entanglement structure is also contained in $\Theta_{12|3}(P)$.

Similarly, we could construct another two polytopes $\Theta_{1|23}(P)$ and $\Theta_{2|13}(P)$ for the partitions $1|23$ and $2|13$, respectively. Denote $\Theta_{2\text{-prod}}(P)$ the convex hull of all the points in $\Theta_{12|3}(P)$, $\Theta_{1|23}(P)$ and $\Theta_{2|13}(P)$. Any mixed 2-producible states must be in $\Theta_{2\text{-prod}}(P)$.

In general, given a partition set Γ and a collection P of non-diagonal elements from a density matrix, Proposition 1 can be employed to derive inequalities that define a convex polytope $\Theta_\gamma(P)$ for each maximum partition γ within Γ , i.e., each partition in Γ^{\max} . The smallest convex polytope that encompasses all $\Theta_\gamma(P)$ is referred to as $\Theta_\Gamma(P)$. The set Γ can be either $\Gamma_{k\text{-prod}}$, $\Gamma_{k\text{-part}}$, or $\Gamma_{k\text{-str}}$, each capturing a distinct aspect of the entanglement structure. The explicit result is summarized as follows.

Theorem 2. *Let $\rho = \sum_i p_i |\psi_i\rangle\langle\psi_i|$ be an N -partite state with $\sum_i p_i = 1$ and $p_i > 0$. If there exists $\xi_i \in \Gamma$ such that $|\psi_i\rangle = \bigotimes_{X_j \in \xi_i} |\psi_{i,X_j}\rangle$ for all $|\psi_i\rangle$, we have*

$$\rho \in \Theta_\Gamma(P), \quad (6)$$

where $\Theta_\Gamma(P)$ is the polytope constructed from a subset of all possible inequalities that can be formulated from Γ^{\max} .

In practice, one can employ the Polyhedra.jl package [43] in Julia to carry out operations on polytope such as intersection and convex hull of several polytopes. An example with the mixed 4-qubit W-state ρ_{W_4} is presented in Section III.D.

B. Criteria based on the hyperplanes

Due to the fact that the computational complexity of the polytope-based criteria increases fastly as the dimension grows, we propose a simplified criterion based on hyperplanes, which offers a more friendly computational approach.

Similar as in Subsection A, we still consider the set of non-diagonal elements $P = \{\rho_{2,3}, \rho_{2,5}, \rho_{3,5}\}$ of a 3-qubit pure quantum state $\rho = |\psi\rangle\langle\psi|$, and the partitions in $\{12|3, 1|23, 2|13\}$. By simply summing up all the inequalities within $\Theta_{12|3}(P)$ in Eq. (5), a unified inequality is created. Similar inequalities can be obtained by applying this method to $\Theta_{2|13}(P)$ and $\Theta_{1|23}(P)$. Those three

new inequalities are as follows:

$$\begin{cases} \sum_{\rho_{m,n} \in P} |\rho_{m,n}| \leq \frac{1}{2}(2\rho_{1,1} + \rho_{6,6} + \rho_{7,7} + \rho_{2,2} + \rho_{3,3}), \\ \sum_{\rho_{m,n} \in P} |\rho_{m,n}| \leq \frac{1}{2}(2\rho_{1,1} + \rho_{4,4} + \rho_{7,7} + \rho_{2,2} + \rho_{5,5}), \\ \sum_{\rho_{m,n} \in P} |\rho_{m,n}| \leq \frac{1}{2}(2\rho_{1,1} + \rho_{4,4} + \rho_{6,6} + \rho_{3,3} + \rho_{5,5}). \end{cases} \quad (7)$$

The right-hand side of the set of inequalities can be formulated as $M \cdot \vec{\beta}^T$, where the row vector $\vec{\beta}$ contains all diagonal elements of ρ , and M is a coefficient matrix. More explicitly,

$$\vec{\beta} = [\rho_{1,1}, \rho_{2,2}, \rho_{3,3}, \rho_{4,4}, \rho_{5,5}, \rho_{6,6}, \rho_{7,7}, \rho_{8,8}],$$

$$M = \begin{bmatrix} 1 & 1/2 & 1/2 & 0 & 0 & 1/2 & 1/2 & 0 \\ 1 & 1/2 & 0 & 1/2 & 1/2 & 0 & 1/2 & 0 \\ 1 & 0 & 1/2 & 1/2 & 1/2 & 1/2 & 0 & 0 \end{bmatrix}.$$

By applying a column-wise maximum operation to matrix M , we obtain a vector $\vec{\alpha}$:

$$\vec{\alpha} = [1 \quad 1/2 \quad 1/2 \quad 1/2 \quad 1/2 \quad 1/2 \quad 1/2 \quad 0].$$

Consequently, we have a new inequality

$$\sum_{\rho_{m,n} \in P} |\rho_{m,n}| \leq \vec{\alpha} \cdot \vec{\beta}^T, \quad (8)$$

which is a relaxation of all the three inequalities in Eq. (7). More explicitly, the new derived criterion is

$$\begin{aligned} & |\rho_{2,3}| + |\rho_{2,5}| + |\rho_{3,5}| \\ & \leq \rho_{1,1} + (\rho_{2,2} + \rho_{3,3} + \rho_{4,4} + \rho_{5,5} + \rho_{6,6} + \rho_{7,7})/2. \end{aligned} \quad (9)$$

In general, for a given set of non-diagonal elements denoted as P and the partition set Γ , we can only consider all the partitions in Γ^{\max} and carry out the same procedure to obtain a new criterion. The main steps are summarized as follows.

1. For each partition $\gamma \in \Gamma^{\max}$, and $\rho_{m,n} \in P$, we obtain from Proposition 1 the inequalities that

$$|\rho_{m,n}| \leq (\rho_{d_{\gamma,1}, d_{\gamma,1}} + \rho_{d_{\gamma,2}, d_{\gamma,2}})/2, \quad (10)$$

where $d_{\gamma,1}$ and $d_{\gamma,2}$ depend on m, n and the partition γ . We remark that there could be different inequalities for the same pair of (m, n) .

2. By choosing one inequality as in Eq. (10) for each $\rho_{m,n} \in P$ and a given partition γ , we obtain

$$\sum_{\rho_{m,n} \in P} |\rho_{m,n}| \leq \vec{m}_\gamma \cdot \vec{\beta}^T, \quad (11)$$

where \vec{m}_γ corresponds to a row in the matrix M .

3. By applying a column-wise maximum operation to matrix M , we obtain a vector $\vec{\alpha}$:

$$\sum_{\rho_{m,n} \in P} |\rho_{m,n}| \leq \vec{\alpha} \cdot \vec{\beta}^T, \quad (12)$$

The partition set Γ can correspond to either $\Gamma_{k\text{-prod}}$, $\Gamma_{k\text{-part}}$ or $\Gamma_{k\text{-str}}$.

Since there could be different options at the second step, the goal to construct the vector $\vec{\alpha}$ is to minimize the sum of all elements in vector $\vec{\alpha}$. To achieve this goal, we can follow the principle to have as many common non-zero columns as possible for each row in the matrix during the construction of M , i.e., the choice of inequality for each pair (m, n) . In other words, we aim to reduce the number of appeared non-zero columns. This strategy helps us to effectively utilize the structure of matrix M while keeping the sum of the elements in vector a minimal. This approach is beneficial for our optimization process.

Further elaboration on the optimization process is provided in Appendix II. The greedy algorithm is implemented to obtain the optimal inequalities, see the codes listed in [44].

The left hand side of the inequality (12) can be replaced by its lower bound $\sum_{\rho_{m,n} \in P} \frac{1}{2}(\rho_{m,n} + \rho_{n,m})$, which can be represented by the expectation value of the observable $W_P = \frac{1}{2}|m\rangle\langle n| + |n\rangle\langle m|$. On the other hand, the right hand side of (12) can be represented the expectation value of the observable $W = \text{diag}\{\vec{\alpha}\}$. Our hyperplane-based criteria is experimentally friendly, which can be implemented by measuring the two observables without state tomography. The two observables can be realized by using local observables and the number of the required local observables scales polynomially with the system size. In comparison, to realize full state tomography, the number of the required local observables grows exponentially.

C. Criteria based on the inner polytopes

An SDP-based method was also developed to create evolving polytopes, whose nodes are different kinds of separable states, for confirming quantum entanglement [41]. Besides, a modified version of Gilbert's algorithm was recently used to solve the convex membership problem [45, 46]. The performance of this SDP-based algorithm depends on the choice of the initial polytope, and the current algorithm generates the initial polytope randomly. As the complexity increases with the increasing system, inspired by the previous works[41, 45, 46], we propose a systematic approach in the following to select the initial polytope so as to guarantee the efficiency and performance.

We introduce a new algorithm to certify the entanglement structure of the mixed state $\rho(t) = t\rho + (1-t)\mathbb{I}_d/d$ for given ρ . Especially, we are interested in the minimal t such that $\rho(t)$ still have the targeted entanglement structure. Our algorithm involves two stages as illustrated in Fig. 2. Different from [41], initially, we employ gradient descent at the first stage, which is followed by SDP at the second stage. The gradient descent is conducted within the Pytorch framework, while the SDP is facilitated through the PICOS [47] library. The whole procedure can be summarized as follows.

1. Initialize an arbitrary polytope \mathcal{P} determined by a set of states $\{\varrho_i\}$ of the entanglement structure corresponding to a partition γ , and a set of probabilities $\{p_i\}$, where $\sum_i p_i = 1$. An example is illustrated in Fig. 2(a).
2. Employing the gradient descent algorithm, we minimize the geometric distance from the state $\varrho = \sum_i p_i \varrho_i$ to the line segment l between ρ and the maximally mixed state, as shown in Fig. 2(b).
A predefined threshold r serves as the criterion for progression to the next step, ensuring a systematic approach to state optimization.
3. Using gradient descent to minimize the geometric distance between the state ϱ and ρ , ensuring that the polytope's boundaries progressively converge to ρ , as illustrated in Fig. 2(c). The optimization process is directed by a loss function $\|\rho - \varrho\| = \sqrt{\text{tr}[(\rho - \varrho)^\dagger(\rho - \varrho)]}$, with the initial polytope configuration determined by the results of step 2. If the distance, as defined in step 2, exceeds the predetermined threshold r , the algorithm reverts to step 2 to ensure that the distance between ϱ and the line segment l remains within the specified limit.

4. Finally, we use SDP to approximate the optimal t_0 . The initial points are chosen as the results in step 3, but we choose one subsystem from each vertex of \mathcal{P} as the unknown one, which is optimized using SDP. Other subsystems except this one from each vertex are denoted as a new set \mathcal{P}' . We do this for each subsystem iteratively. The details of the SDP are as follows:

$$\begin{aligned} & \max t \\ & \text{w.r.t. } t, \tau_i \succcurlyeq 0 \\ & \text{s.t. } \rho(t) = \sum_{\varrho_i \in \mathcal{P}'} \varrho_i \otimes \tau_i, \end{aligned} \quad (13)$$

where the trace of τ_i is not necessarily one.

While step 2 permits the convergence of ϱ towards the line segment l , the intersection of the polytope \mathcal{P} with

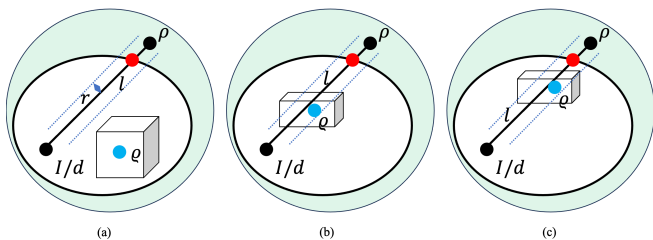


FIG. 2. (a) Initialise an arbitrary polytope $\mathcal{P} = \{\varrho_i\}$ and $\varrho = \sum_i P_i \varrho_i$. (b) Minimize the distance between the quantum state ϱ and the segment l . (c) Minimize the distance between the quantum state ϱ and ρ .

l , and consequently the feasibility of SDP, cannot be assured. To improve on this point, we optimize the quantum subsystems corresponding to the largest partition of each node via SDP at each iteration. For fully separable states and certain entanglement structures where SDP is infeasible, we can also construct an initial polytope using only states derived from mutually-unbiased bases (MUBs), which not only covers a substantial volume but also encapsulate the maximally mixed state. More explicitly for the case that the local dimension is 2, the constraint condition in Eq. (13) transforms into the following expression:

$$\rho(t) = \sum_{\varrho_i \in (\mathcal{P}' \cup \mathcal{P}_{N-1})} \varrho_i \otimes \tau_i,$$

where \mathcal{P}_{N-1} is defined as follows:

$$\left\{ \bigotimes_{i=1}^{N-1} \rho_i, \rho_i \in \left\{ \frac{(\mathbb{I}_2 \pm \sigma_x)}{2}, \frac{(\mathbb{I}_2 \pm \sigma_y)}{2}, \frac{(\mathbb{I}_2 \pm \sigma_z)}{2} \right\} \right\}. \quad (14)$$

Since \mathcal{P}_{N-1} contains the maximally mixed state, the feasibility of SDP can be guaranteed.

D. Applications of method with inner polytopes

Firstly, we study the full separability of the states $\rho(t) = t\rho + (1-t)\mathbb{I}_d/d$, where ρ is any state up to six qubits. The results are computed by the algorithm based on the inner polytope. We compare the results with the known ones in the literature in Table I.

For the 4 qubit, 5-qubit and 6-qubit noisy GHZ states, the results computed by our algorithm based on the inner polytope give the necessary and sufficient values of the full separability, which are 1/9, 1/17 and 1/33, respectively [14]. Our method performs better compared with the algorithm in [41] in most cases.

Then, we utilize our algorithm based on the inner polytope to compute the entanglement partitionability and the entanglement producibility of $\rho(t)$ with ρ to be 4-qubit W state, 4-qubit and 5-qubit GHZ states in Tables II, III and IV as follows.

TABLE I. Comparison of the full separability computed by our method and the ones by adaptive polytopes [41]. The “-” in the table signifies that [41] either did not provide the results or the code provided by [41] was unable to perform the calculations.

Quantum States	Our result	Lower bound of [41]
GHZ(6 Qubits)	0.030303	-
W(6 Qubits)	0.02345	-
Cluster state (6 Qubits)	0.030303	-
GHZ(5 Qubits)	0.05882	0.05878
W(5 Qubits)	0.047084	0.046956
Cluster state (5 Qubits)	0.05882	-
GHZ(4 Qubits)	0.1111	0.1111
W(4 Qubits)	0.0926	0.0926
Cluster state (4 Qubits)	0.1111	0.1111
Dicke (4 Qubits, 2 ex.)	0.085708	0.08571

TABLE II. Comparison of the partitionability and the producibility computed by our algorithm and the known ones in the literature for the mixture of 4-qubit W state and white noise.

Entanglement Structure	Our result	Other known results
3-part	0.247	0.243[45]
2-prod	0.247	0.245[45]
2-part	0.4705	0.474[8]

Table II shows that our results based on inner polytope perform better than the results in [45] in most cases for 4-qubit noisy W state. Table III shows the bound corresponding to 3-partitionability is 0.19997 for 4-qubit noisy GHZ state, which approaches the necessary and sufficient value $p = 0.2$ [14]. Besides, the bound 0.2725 for 2-producibility is better than the one in [45].

Table IV is for 5-qubit noisy GHZ state. Our results of 2/3/4-partitionability are very close to the optimal known values given in [14]. For the producibility, our results are better compared with the ones in [45]. From [17] the exact bound is no more than 0.238 for 2-producibility of $\rho(t)$, which is close to our bound 0.2375.

Besides, our algorithm can provide the exact decomposition of k -partitionable (producible, or stretchable) states. By calculation the fidelity between the state $\rho(t)$ and the decomposition of the state obtained by our algorithm is 99.999%. Thus the precision of our algorithm is guaranteed.

Furthermore, we can detect the entanglement structure of any state ρ mixed with any fully separable states. For example, we consider $\rho(t) = t|W\rangle\langle W| + (1-t)\rho_f$, where $|W\rangle = (|0001\rangle + |0010\rangle + |0100\rangle + |1000\rangle)/2$ and $\rho_f = \bigotimes_{i=1}^4 \tau_i$ with $\tau_i = (3|0\rangle\langle 0| + |1\rangle\langle 1|)/4$. Our algorithm

TABLE III. Comparison of the partitionability and the producibility computed by our algorithm and the known ones in the literature for the mixture of 4-qubit GHZ state and white noise.

Entanglement Structure	Our result	Other known results
3-part	0.19997	0.198[45]
2-prod	0.27251	0.269[45]
2-part	0.46456	0.467[8](exact)

TABLE IV. Comparison of the partitionability and the producibility computed by our algorithm and the known ones in the literature for the mixture of 5-qubit GHZ state and white noise.

Entanglement Structure	Our result	Other known Results
4-part	0.09434	0.0943 [14]
2-prod	0.2375	0.19[45]
3-part	0.2377	0.2380[14]
3-prod	0.3846	0.278[45]
2-part	0.48378	0.4839[14]

shows that $\rho(t)$ is fully separable when $t < 0.1468$ and 2-partitionable if $t < 0.58$, while $\rho(t)$ is fully separable when $t < 0.1464$ and 2-partitionable for $t < 0.5623$ in [45].

To guarantee the universality of our algorithm, in our algorithm the initial states are optimized by the gradient conjugate method. We only optimize one partite states, given that the other partite states are initialized. In this way, the runtime of our algorithm could be slightly longer than that in [41].

E. Applications of method with hyperplane

To illustrate our results by the witness based on the hyperplane, we give the following examples.

Example 1. Consider the family of 4-qubit quantum states,

$$\rho_{W_4} = (1-t)\frac{\mathbb{I}}{2^4} + t|W_4\rangle\langle W_4|,$$

with $|W_4\rangle = \frac{1}{2}(|0001\rangle + |0010\rangle + |0100\rangle + |1000\rangle)$.

We select P as the one given in Appendix III and obtain that if ρ is 2-producible or 3-partitionable, 0-stretchable or (-1) -stretchable, the entries of ρ fulfill the following inequality,

$$\frac{1}{2}|\text{Tr}[W_P \cdot \rho]| \leq \text{Tr}[W_{2\text{-prod}} \cdot \rho], \quad (15)$$

where W_P select the targeted off-diagonal elements of ρ , and $W_{2\text{-prod}} = \text{diag}\{a_1, \dots\}$ is the diagonal matrix with

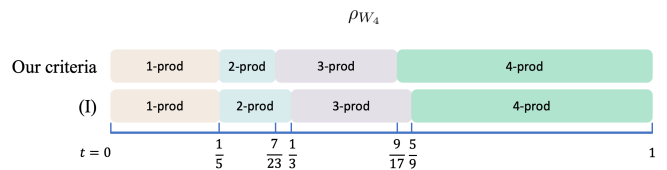


FIG. 3. The illustration shows the results obtained by using our criteria and Theorem 2 of Ref. [17]((I) in the figure). to detect the entanglement depth.

$a_1 = 2$ and $a_2 = a_3 = a_4 = a_5 = a_6 = a_7 = a_9 = a_{10} = a_{11} = a_{13} = 1/2$.

If ρ is 3-producible or 2-partitionable, the entries of ρ satisfy

$$\frac{1}{2}|\text{Tr}[W_P \cdot \rho]| \leq \text{Tr}[W_{3\text{-prod}} \cdot \rho], \quad (16)$$

where $W_{3\text{-prod}} = \text{diag}\{a_1, \dots\}$ is the diagonal matrix with $a_1 = 2$, $a_2 = a_3 = a_5 = a_9 = 1$ and $a_4 = a_6 = a_7 = a_{10} = a_{11} = a_{13} = 1/2$. The witness in [38] can detect 2 (3 and 4)-partite entanglement when $p > 0.592$ ($p > 0.729$ and $p > 0.873$) while our theorem can detect 2 (3 and 4)-partite entanglement when $p > 0.2$ ($p > 0.304$ and $p > 0.529$). The results compared with the best result so far in [17] are illustrated in Fig. 3. The details can be found in Appendix III.

Example 2. Now we consider the family of 4-qutrit quantum states,

$$\rho(p, q) = p|W\rangle\langle W| + q\sigma^{\otimes 4}|W\rangle\langle W| + \frac{1-p-q}{3^4}\mathbb{I},$$

where $|W\rangle = \frac{1}{2\sqrt{2}}(\sum_{i=1}^2 |i000\rangle + |0i00\rangle + |00i0\rangle + |000i\rangle)$, and $\sigma|0\rangle = |1\rangle$, $\sigma|1\rangle = |2\rangle$, $\sigma|2\rangle = |0\rangle$. When $p > 14(1-q)/95$ and $q > 14(1-p)/95$, the two inequalities (23) in Appendix III are violated and ρ is genuinely 3-partite entangled. The results are compared with the ones in [17], which are the best results so far in FIG. 4.

For the W states mixed with white noise in Example 1 and Example 2, our inequalities perform also better compared with the results in [17].

Example 3. Consider the 5-qubit mixed states,

$$\rho_{CL_5^s} = (1-t)\frac{\mathbb{I}}{2^5} + t|CL_5^s\rangle\langle CL_5^s|,$$

where $|CL_5^s\rangle = \frac{1}{2}(|00000\rangle + |01111\rangle + |10011\rangle + |11100\rangle)$.

The results are illustrated in Fig. 5, see also the details given in Appendix III. The results in [23] show that $\rho_{CL_5^s}$ is not 5-partitionable (4- or 3-partitionable) when $t > 7/13$ while the ones by our criteria are $t > 1/9$ ($t > 5/29$ or $t > 9/25$), and $\rho_{CL_5^s}$ is 2-partitionable or genuine multipartite entangled when $t > 9/13$, while $t > 13/29$ by our method.

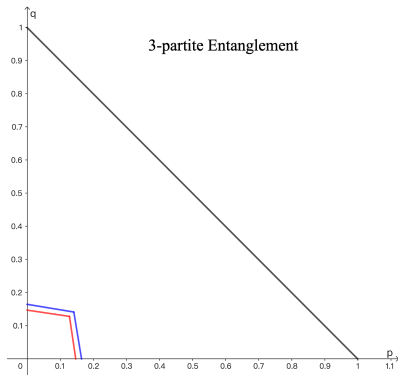


FIG. 4. The red line consists of the line $q = \frac{14}{95}(1 - p)$, $p \in [0, \frac{14}{109}]$ and the line $p = \frac{14}{95}(1 - q)$, $q \in [0, \frac{14}{109}]$. The area enclosed by the red line, p axis, line $q = 1 - p$ and the q axis corresponds to the quantum states containing genuine 3-partite entanglement detected by our Theorem II. The blue line consists of the line $q = \frac{16}{97}(1 - p)$, $p \in [0, \frac{16}{113}]$ and the line $p = \frac{16}{97}(1 - q)$, $q \in [0, \frac{16}{113}]$. The area enclosed by the blue line, p axis, line $q = 1 - p$ and the q axis corresponds to the quantum states containing genuine 3-partite entanglement detected by the Theorem 2 of Ref.[17].

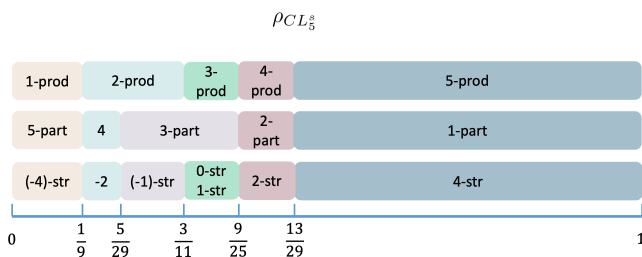


FIG. 5. Illustration of the results obtained by using our criteria in detecting the entanglement depth and intactness of $\rho_{CL_5^s}$.

Example 4. Consider the 6-qubit mixed states,

$$\rho_{GHZ_6} = (1 - t) \frac{\mathbb{I}}{2^6} + t |GHZ_6\rangle\langle GHZ_6|,$$

where $|GHZ_6\rangle = \frac{1}{\sqrt{2}}(|000000\rangle + |111111\rangle)$.

In this case, the witness in [38] can detect 2-partitional entanglement only when $t > 32/63$, the genuine entanglement only when $p > 31/47$, 2 (3,4,5 and 6)-partite entanglement when $t > 0.366$ ($t > 0.448, p > 0.522, 0.556$ and $p > 0.649$). The witness in [23] can only detect the genuine multipartite entanglement of ρ_{GHZ_6} when $p > 31/47$. While our criteria can detect the genuine entanglement when $p > 31/63$, and 2(3,4, and 5)-partite entanglement when $p > 1/33$ ($p > 5/37, p > 15/47$, and $p > 25/57$). The results are compared with the ones in [17], which are the best known results so far, see Fig. 6 in page 8 and further details are given in Appendix III. Our algorithm can detect more entangled regions compared with the previous ones.

Our criteria based on the hyperplane can detect more k -partitionable, k -producible and k -stretchable states compared with the previous analytical results, and can be implemented experimentally by measuring local observables. Take 6-qubit GHZ state mixed with white noise, W^P can be realized by using 32 local observables. To detect the k -nonseparable states, the observable $W_{k\text{-part}}$ can be realized using 4 (34, 14, 14, 4) local observables for $k = 2$ (3, 4, 5, 6), respectively. To detect the k -partite states, the observable $W_{k\text{-prod}}$ can be realized by using 4(12, 32, 16, 4) local observables for $k = 2$ (3, 4, 5, 6), respectively.

IV. CONCLUSION

Based on the property that all states with the same entanglement structure constitute a convex set, we have designed an algorithm by using SDP and the gradient descent method to approximate the convex set from the inside of it. The gradient descent method optimizes the initial points for the SDP, thus the probability to obtain the global optimum is increased. And we have also constructed the criteria from the outer polytopes of the convex set to characterize the multipartite entanglement structure. These criteria can be implemented through local observables and the number of the ones grows linearly with the system size. The criteria can be optimized further by optimizing the selection of the off-diagonal elements and diagonal elements of the density matrices. The algorithms and the criteria can characterize the multipartite entanglement structure better compared with existing criteria.

ACKNOWLEDGEMENTS This work is supported by the Fundamental Research Funds for the Central Universities; the National Natural Science Foundation of China (NSFC) under Grants 12071179, 12305007, 12371132, 12075159 and 12171044; Anhui Provincial Natural Science Foundation (Grant No. 2308085QA29); the Alexander von Humboldt Foundation; Natural Science Foundation of Shanghai (Grant No. 20ZR1426400); Shenzhen Institute for Quantum Science and Engineering, Southern University of Science and Technology (Grant Nos. SIQSE202005); the Academician Innovation Platform of Hainan Province.

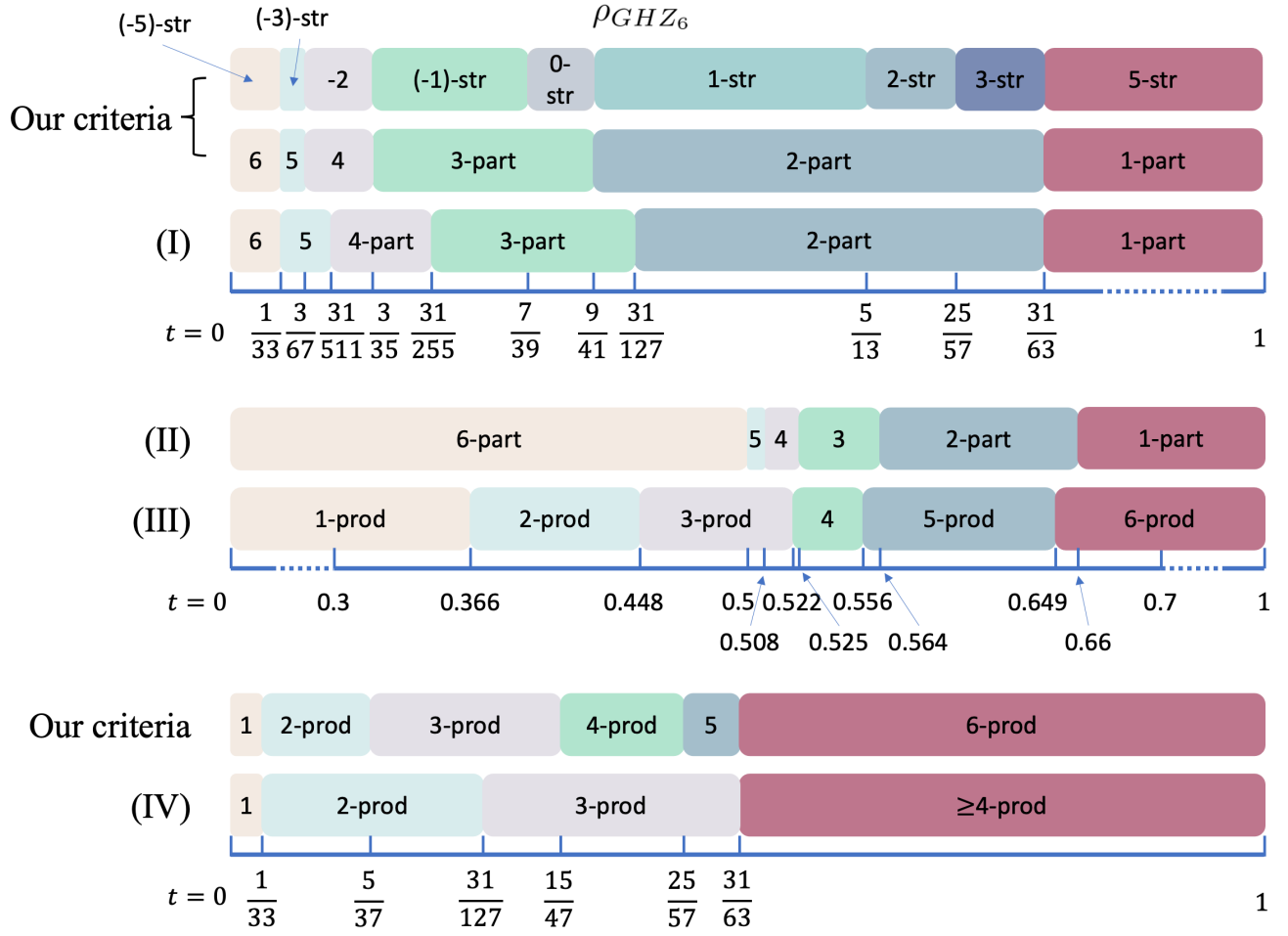


FIG. 6. Illustration of the results obtained by using our criteria in detecting the k -partitionability and k -productibility of ρ_{GHZ_6} . In the figure, (I) showcases the results derived from Theorem 3 of Ref. [17], (IV) presents the results from Theorem 1 of Ref. [17], (II) demonstrates the results based on Equation A25 of Ref. [38], and (III) illustrates the results based on Equation A31 of Ref. [38].

V. APPENDIX I

The proof of Proposition 1 is given as follows.

Proof of Proposition 1

$$\begin{aligned}
& |\langle m|\psi\rangle\langle\psi|n\rangle| = \sqrt{\langle m|\psi\rangle\langle\psi|n\rangle\langle n|\psi\rangle\langle\psi|m\rangle} \\
& = \sqrt{\langle m_{X_i}|\langle m_{\bar{X}_i}| \rangle|\psi_{X_i}\rangle|\psi_{\bar{X}_i}\rangle} \times \sqrt{\langle\psi_{X_i}|\langle\psi_{\bar{X}_i}| \rangle(|n_{X_i}\rangle|n_{\bar{X}_i}\rangle)} \times \sqrt{\langle n_{X_i}|\langle n_{\bar{X}_i}| \rangle|\psi_{X_i}\rangle|\psi_{\bar{X}_i}\rangle} \times \sqrt{\langle\psi_{X_i}|\langle\psi_{\bar{X}_i}| \rangle(|m_{X_i}\rangle|m_{\bar{X}_i}\rangle)} \\
& = \sqrt{\langle m_{X_i}|\psi_{X_i}\rangle\langle m_{\bar{X}_i}|\psi_{\bar{X}_i}\rangle} \times \sqrt{\langle\psi_{X_i}|n_{X_i}\rangle\langle\psi_{\bar{X}_i}|n_{\bar{X}_i}\rangle} \times \sqrt{\langle n_{X_i}|\psi_{X_i}\rangle\langle n_{\bar{X}_i}|\psi_{\bar{X}_i}\rangle} \times \sqrt{\langle\psi_{X_i}|m_{X_i}\rangle\langle\psi_{\bar{X}_i}|m_{\bar{X}_i}\rangle} \\
& = \sqrt{\langle m_{X_i}|\psi_{X_i}\rangle\langle n_{\bar{X}_i}|\psi_{\bar{X}_i}\rangle} \times \sqrt{\langle\psi_{X_i}|m_{X_i}\rangle\langle\psi_{\bar{X}_i}|n_{\bar{X}_i}\rangle} \times \sqrt{\langle n_{X_i}|\psi_{X_i}\rangle\langle m_{\bar{X}_i}|\psi_{\bar{X}_i}\rangle} \times \sqrt{\langle\psi_{X_i}|n_{X_i}\rangle\langle\psi_{\bar{X}_i}|m_{\bar{X}_i}\rangle} \\
& = \sqrt{(\langle m_{\bar{X}_i}|\langle n_{X_i}| \rangle|\psi\rangle\langle\psi|(|m_{\bar{X}_i}\rangle|n_{X_i}\rangle)} \times \sqrt{(\langle m_{X_i}|\langle n_{\bar{X}_i}| \rangle|\psi\rangle\langle\psi|(|m_{X_i}\rangle|n_{\bar{X}_i}\rangle)} \\
& \leq \frac{1}{2}[(\langle m_{\bar{X}_i}|\langle n_{X_i}| \rangle|\psi\rangle\langle\psi|(|m_{\bar{X}_i}\rangle|n_{X_i}\rangle) + (\langle m_{X_i}|\langle n_{\bar{X}_i}| \rangle|\psi\rangle\langle\psi|(|m_{X_i}\rangle|n_{\bar{X}_i}\rangle)].
\end{aligned}$$

VI. APPENDIX II

In the following part, we illustrate the optimization process for the inequality based on outer polytopes. The left-hand side of the inequality represents the sum of the absolute values of the non-diagonal elements in P , while the right-hand side is the inner product of the vectors $\vec{\alpha}$ and $\vec{\beta}$. $\vec{\alpha}$ is derived from the coefficient matrix M by taking the maximum value of per column. The entire optimization process can be viewed as the optimization of a combination of inequalities.

The optimization strategy adheres to two fundamental principles: (1) Maximize the number of all zero columns within matrix M . (2) Minimize the sum of the elements comprising the vector $\vec{\alpha}$.

For each element $\rho_{m,n}$ within the set P , at least one corresponding inequality can be formulated for every partition γ_i . We denote the set of the inequalities with respect to $\rho_{m,n}$ and γ_i as $S_{m,n}^{\gamma_i}$. We construct a candidate set from the inequalities in $S_{m,n}^{\gamma_i}$ for all $\gamma_i \in \Gamma^{max}$ and given ρ_{mn} , which satisfies two conditions: (1) containing one inequality for every partition, (2) containing as few inequalities as possible. It is acknowledged that there are multiple such sets that could fulfill these conditions. Based on the principle of minimizing the number of diagonal elements on the right-hand side of the inequalities, an optimal candidate set $S_{m,n}$ is selected for each element $\rho_{m,n}$ from the set P .

Then the given partition γ_i and each element $\rho_{m,n}$ and we select one inequality from the set $S_{m,n}^{\gamma_i} \cap S_{m,n}$ and then we add the left and the right hand sides of all the inequalities respectively for m and n , the inequality corresponding to the i -th row of M is attained. The selection principle is minimizing the summation of the elements that

comprise the vector $\vec{\alpha}$, The details of the selecting are as follows.

There may exist a specific partition γ such that for each part X_i within γ , it holds that $|m_{X_i}\rangle = |n_{X_i}\rangle$. This implies that for $\rho_{m,n}$, the corresponding inequality associated with partition γ is $|\rho_{m,n}| \leq (\rho_{m,m} + \rho_{n,n})/2$, which is trivial from the positive definiteness of the density matrices. For each partition γ_i in Γ^{max} , all trivial inequalities associated with γ_i can be determined. By summing the left and the right hand sides of these trivial inequalities respectively, we can obtain the corresponding trivial inequality for γ_i .

The right-hand side of the trivial inequalities for all partitions in Γ^{max} can also be expressed as the inner product of a matrix M' with the vector $\vec{\beta}$. Subsequently, by taking the maximum value across the columns of M' , we obtain the vector $\vec{\eta}$. The maximum values in all columns of matrix M , which correspond to all trivial inequalities, are determined by $\vec{\eta}$. The vector $\vec{\eta}$ can be considered as the zeroth row of the matrix M . Then, when constructing a certain row of the matrix M , if the value in the zeroth row of a certain column is not equal to zero, and the value in that row and column of M is smaller than the value in the zeroth row, it may be beneficial to adjust the selection of inequalities such that the value in that row and column approaches the value in the zeroth row. This approach aligns well with our guiding principle for selection. This process involves exact matching, for which we have utilized the Dancing Links algorithm [48]. An illustration of this approach will be provided in the forthcoming details of Example 1. All of the aforementioned constitutes our comprehensive optimization strategies and techniques.

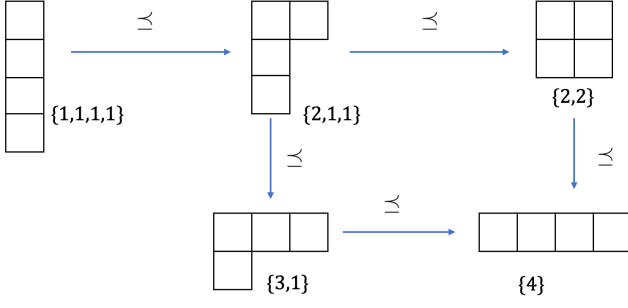


FIG. 7. The types of all partitions of the set $\{1, 2, 3, 4\}$ are represented by Young diagrams, along with their poset relationships.

VII. APPENDIX III

In the following section, we give the details to detect the entanglement structure of the examples using the criteria based on the outerplane. To represent the partitions for short in the examples, we give the definitions of the type of the partitions firstly. The type of the partition γ (the integer partition of N) is denoted as $\hat{\gamma} = \{|X_1|, \dots, |X_{|\gamma|}|\}$, where X_i is the part of γ . Disregarding the sequence of elements, the type of the partition γ is uniquely identified. $\hat{\gamma}$ is the refinement of $\hat{\xi}$ if γ is the refinement of ξ . as depicted in Fig. 7, Young diagrams provide a graphical representation for the types of partitions. If $\hat{\gamma}$ is the refinement of $\hat{\xi}$, then for each partition γ_1 in $\hat{\gamma}$, there exists a partition ξ_1 in $\hat{\xi}$ such that $\gamma_1 \preceq \xi_1$.

For example, as depicted in Fig. 7, when we consider the set of partition types for $\Gamma_{2\text{-part}}$ of $\{1, 2, 3, 4\}$, we find that it consists of $\{\{1, 1, 1, 1\}, \{2, 1, 1\}, \{2, 2\}, \{3, 1\}\}$. Among these, the maximal elements within the set of partition types are $\{\{2, 2\}, \{3, 1\}\}$. Consequently, $\Gamma_{2\text{-part}}^{\max}$ encompasses all partitions whose types are either $\{2, 2\}$ or $\{3, 1\}$, reflecting the partitions that achieve the greatest refinement within the poset defined by $\Gamma_{2\text{-part}}$.

Then we illustrated the details of the Examples in E of Section III.

The details of Example 1:

We select the set of non-diagonal elements $P = \{\rho_{2,3}, \rho_{2,5}, \rho_{2,9}, \rho_{3,5}, \rho_{3,9}, \rho_{5,9}\}$.

The sets of maximal elements of all k -stretchable partitions of $\{1, 2, 3, 4\}$ are

$$\begin{aligned} \Gamma_{(-1)\text{-str}}^{\max} &= \{12|3|4, 13|2|4, 14|2|3, 23|1|4, 24|1|3, 34|1|2\}, \\ \Gamma_{0\text{-str}}^{\max} &= \{12|34, 13|24, 14|23\}, \\ \Gamma_{1\text{-str}}^{\max} &= \Gamma_{0\text{-str}}^{\max} \cup \{123|4, 124|3, 134|2, 234|1\}. \end{aligned}$$

If ρ is 3-partitionable or (-1) -stretchable, the trivial inequality corresponding to $12|3|4$ is $|\rho_{5,9}| \leq (\rho_{5,5} +$

$\rho_{9,9})/2$. Additionally, the trivial inequality corresponding to $12|3|4$ is $|\rho_{2,3}| \leq (\rho_{2,2} + \rho_{3,3})/2$. As a result, the vector $\vec{\eta} = [\eta_1, \eta_2, \dots, \eta_{16}]$ can be defined with $\eta_2 = \eta_3 = \eta_5 = \eta_9 = 1/2$. When constructing the inequality corresponding to $1|2|3|4$, if we select $|\rho_{5,9}| \leq (\rho_{1,1} + \rho_{13,13})/2$, the coefficient of $\rho_{1,1}$ in the final inequality becomes 2.5. However, if we select $|\rho_{5,9}| \leq (\rho_{5,5} + \rho_{9,9})/2$, it appears to add a trivial inequality, but the coefficient of $\rho_{1,1}$ in the final inequality becomes 2, with no change in the coefficients of other terms. This is the optimization method for adjusting inequality selection introduced in Appendix II.

Therefore, if ρ is 3-partitionable or (-1) -stretchable, the partition $12|3|4$ and $34|1|2$ correspond to the following inequality:

$$\begin{aligned} \sum_{\rho_{m,n} \in P} |\rho_{m,n}| \leq & 2\rho_{1,1} + \frac{1}{2}(\rho_{6,6} + \rho_{7,7} + \rho_{10,10} + \rho_{11,11} \\ & + \rho_{2,2} + \rho_{3,3} + \rho_{5,5} + \rho_{9,9}), \end{aligned} \quad (17)$$

and the partition $13|2|4$ and $24|1|3$ correspond to the following inequality:

$$\begin{aligned} \sum_{\rho_{m,n} \in P} |\rho_{m,n}| \leq & 2\rho_{1,1} + \frac{1}{2}(\rho_{4,4} + \rho_{7,7} + \rho_{10,10} + \rho_{13,13} \\ & + \rho_{2,2} + \rho_{3,3} + \rho_{5,5} + \rho_{9,9}), \end{aligned} \quad (18)$$

and the partition $14|2|3$ and $23|1|4$ correspond to the following inequality:

$$\begin{aligned} \sum_{\rho_{m,n} \in P} |\rho_{m,n}| \leq & 2\rho_{1,1} + \frac{1}{2}(\rho_{4,4} + \rho_{6,6} + \rho_{11,11} + \rho_{13,13} \\ & + \rho_{2,2} + \rho_{3,3} + \rho_{5,5} + \rho_{9,9}). \end{aligned} \quad (19)$$

Thus one of the criteria is

$$\begin{aligned} \sum_{\rho_{m,n} \in P} |\rho_{m,n}| \leq & 2\rho_{1,1} + \frac{1}{2}(\rho_{4,4} + \rho_{6,6} + \rho_{7,7} + \rho_{10,10} + \rho_{11,11} \\ & + \rho_{13,13} + \rho_{2,2} + \rho_{3,3} + \rho_{5,9} + \rho_{9,9}). \end{aligned} \quad (20)$$

If ρ is 2-producible or 0-stretchable, the partition $12|3|4$ corresponds to the inequality (17), and the partition $13|2|4$ corresponds to the inequality (18), and the partition $14|2|3$ corresponds to the inequality (19). Thus one of the criteria is the inequality (20).

If ρ is 3-producible, 2-partitionable, or 1-stretchable, one of the criteria is

$$\begin{aligned} \sum_{\rho_{m,n} \in P} |\rho_{m,n}| \leq & 2\rho_{1,1} + \frac{1}{2}(\rho_{4,4} + \rho_{6,6} + \rho_{7,7} + \rho_{10,10} + \rho_{11,11} \\ & + \rho_{13,13}) + (\rho_{2,2} + \rho_{3,3} + \rho_{5,9} + \rho_{9,9}). \end{aligned} \quad (21)$$

The observable W_P and $W_{k\text{-prod}}$ in the left and right hand sides of the inequalities in this example can be expressed as

$$\begin{aligned} W_P &= \sum_{1 \leq i < j \leq n} [(\bigotimes_{k \neq i,j} Z_k^+) \otimes H_{i,j}], \\ W_{2\text{-prod}} &= 2\Delta_1 + \frac{1}{2}(\Delta_2 + \Delta_3) \\ W_{3\text{-prod}} &= 2\Delta_1 + \Delta_2 + \frac{1}{2}\Delta_3 \end{aligned} \quad (22)$$

with

$$\begin{aligned} Z_i^+ &= \frac{(\mathbb{I}_2 + \sigma_z^{(i)})}{2}, Z_i^- = \frac{(\mathbb{I}_2 - \sigma_z^{(i)})}{2}, \\ H_i^+ &= |0\rangle_i \langle 1|, H_i^- = |1\rangle_i \langle 0| \\ H_{i,j} &= H_i^+ \otimes H_j^- + H_i^- \otimes H_j^+ \\ \Delta_1 &= \bigotimes_{i=1}^4 Z_k^+ \\ \Delta_2 &= \sum_{i=1}^4 Z_i^- \otimes \left[\bigotimes_{j=1, j \neq i}^4 Z_j^+ \right] \\ \Delta_3 &= \sum_{1 \leq i_1 < i_2 \leq 4} Z_{i_1}^+ \otimes Z_{i_2}^+ \otimes \left[\bigotimes_{j \neq i_1, i_2} Z_j^- \right] \end{aligned}$$

and $\sigma_z^{(i)}$ being the pauli matrix of the i -th system.

The details of Example 2.

We select $P_1 = \{ \rho_{2,3}, \rho_{2,4}, \rho_{2,7}, \rho_{2,10}, \rho_{2,19}, \rho_{2,28}, \rho_{2,55}, \rho_{3,4}, \rho_{3,7}, \rho_{3,10}, \rho_{3,19}, \rho_{3,28}, \rho_{3,55}, \rho_{4,7}, \rho_{4,10}, \rho_{4,19}, \rho_{4,28}, \rho_{4,55}, \rho_{7,10}, \rho_{7,19}, \rho_{7,28}, \rho_{7,55}, \rho_{10,19}, \rho_{10,28}, \rho_{10,55}, \rho_{19,28}, \rho_{19,55}, \rho_{28,55} \}$, and $P_2 = \{ \rho_{14,32}, \rho_{14,38}, \rho_{14,40}, \rho_{14,42}, \rho_{14,44}, \rho_{14,50}, \rho_{14,68}, \rho_{32,38}, \rho_{32,40}, \rho_{32,42}, \rho_{32,44}, \rho_{32,50}, \rho_{32,68}, \rho_{38,40}, \rho_{38,42}, \rho_{38,44}, \rho_{38,50}, \rho_{38,68}, \rho_{40,42}, \rho_{40,44}, \rho_{40,50}, \rho_{40,68}, \rho_{42,44}, \rho_{42,50}, \rho_{42,68}, \rho_{44,50}, \rho_{44,68}, \rho_{50,68} \}$.

If ρ is 2-producible, then

$$\sum_{\rho_{m,n} \in P_i} |\rho_{m,n}| \leq \text{Tr}[W_{2\text{-prod}}^{P_i} \cdot \rho], \quad (23)$$

where $W_{2\text{-prod}}^{P_i} = \text{diag}\{a_1^i, \dots\}$ ($i = 1, 2$) is the diagonal matrix with $a_1^1 = 8, a_2^1 = a_3^1 = a_4^1 = a_7^1 = a_{10}^1 = a_{19}^1 = a_{28}^1 = a_{55}^1 = 1$ and $a_5^1 = a_6^1 = a_8^1 = a_9^1 = a_{11}^1 = a_{12}^1 = a_{13}^1 = a_{16}^1 = a_{20}^1 = a_{21}^1 = a_{22}^1 = a_{25}^1 = a_{29}^1 = a_{30}^1 = a_{31}^1 = a_{34}^1 = a_{37}^1 = a_{46}^1 = a_{56}^1 = a_{57}^1 = a_{58}^1 = a_{61}^1 = a_{64}^1 = a_{73}^1 = \frac{1}{2}$. and $a_{41}^2 = 8, a_{14}^2 = a_{32}^2 = a_{38}^2 = a_{40}^2 = a_{42}^2 = a_{44}^2 = a_{50}^2 = a_{68}^2 = 1$ and $a_5^2 = a_{11}^2 = a_{13}^2 = a_{15}^2 = a_{17}^2 = a_{23}^2 = a_{28}^2 = a_{31}^2 = a_{33}^2 = a_{35}^2 = a_{37}^2 = a_{39}^2 = a_{43}^2 = a_{45}^2 = a_{47}^2 = a_{49}^2 = a_{51}^2 = a_{53}^2 = a_{59}^2 = a_{65}^2 = a_{67}^2 = a_{69}^2 = a_{71}^2 = a_{77}^2 = \frac{1}{2}$.

The observable $W_{P_1}, W_{P_2}, W_{2\text{-prod}}^{P_1}$ and $W_{2\text{-prod}}^{P_2}$ in the left and right hand sides of the inequalities in this example can be expressed as

$$\begin{aligned} W_{P_1} &= \sum_{1 \leq i < j \leq 4} [(\bigotimes_{k \neq i,j} Z_k^0) \otimes (H_{i,j} + J_{i,j} + \Delta_{i,j}^1 + \Delta_{j,i}^1)] \\ W_{P_2} &= \sum_{1 \leq i < j \leq 4} [(\bigotimes_{k \neq i,j} Z_k^1) \otimes (H_{i,j} + K_{i,j} + \Delta_{i,j}^2 + \Delta_{j,i}^2)] \\ W_{2\text{-prod}}^{P_1} &= 8 \cdot \left(\bigotimes_{i=1}^4 Z_i^0 \right) + \frac{1}{2} \sum_{1 \leq i < j \leq 4} [(\sum_{a,b \in \{1,2\}} Z_i^a \otimes Z_j^b) \\ &\quad \otimes (\bigotimes_{k \neq i,j} Z_k^0)] + \sum_{1 \leq i \leq 4} [(\bigotimes_{k \neq i} Z_k^0) \otimes (Z_i^1 + Z_i^2)] \\ W_{2\text{-prod}}^{P_2} &= 8 \cdot \left(\bigotimes_{i=1}^4 Z_i^1 \right) + \frac{1}{2} \sum_{1 \leq i < j \leq 4} [(\sum_{a,b \in \{0,2\}} Z_i^a \otimes Z_j^b) \\ &\quad \otimes (\bigotimes_{k \neq i,j} Z_k^1)] + \sum_{1 \leq i \leq 4} [(\bigotimes_{k \neq i} Z_k^1) \otimes (Z_i^0 + Z_i^2)] \end{aligned} \quad (24)$$

with

$$\begin{aligned} Z_i^0 &= |0\rangle_i \langle 0|, Z_i^1 = |1\rangle_i \langle 1|, Z_i^2 = |2\rangle_i \langle 2| \\ H_i^+ &= |0\rangle_i \langle 1|, H_i^- = |1\rangle_i \langle 0| \\ J_i^+ &= |0\rangle_i \langle 2|, J_i^- = |2\rangle_i \langle 0| \\ K_i^+ &= |1\rangle_i \langle 2|, K_i^- = |2\rangle_i \langle 1| \\ H_{i,j} &= H_i^+ \otimes H_j^- + H_i^- \otimes H_j^+ \\ J_{i,j} &= J_i^+ \otimes J_j^- + J_i^- \otimes J_j^+ \\ K_{i,j} &= K_i^+ \otimes K_j^- + K_i^- \otimes K_j^+ \\ \Delta_{i,j}^1 &= H_i^+ \otimes J_j^- + H_i^- \otimes J_j^+ \\ \Delta_{i,j}^2 &= H_i^+ \otimes K_j^- + H_i^- \otimes K_j^+ \end{aligned} \quad (25)$$

The details of Example 3.

Unless otherwise specified, we select $P = \{\rho_{1,16}, \rho_{1,20}, \rho_{1,29}, \rho_{16,20}, \rho_{16,29}, \rho_{20,29}\}$.

If ρ is (-2) -stretchable or 4-partitionable, $\Gamma_{4\text{-part}}^{\max}$ is a set of partitions having the type $\{2, 1, 1, 1\}$. By the greedy algorithm, one of the criteria is

$$\sum_{\rho_{m,n} \in P} |\rho_{m,n}| \leq \text{Tr}[W_{4\text{-part}} \cdot \rho], \quad (26)$$

where $W_{4\text{-part}} = \text{diag}\{a_1, \dots\}$ is the diagonal matrix with $a_2 = a_3 = a_4 = a_5 = a_8 = a_9 = a_{12} = a_{13} = a_{14} = a_{15} = a_{17} = a_{18} = a_{19} = a_{21} = a_{24} = a_{25} = a_{28} = a_{30} = a_{31} = a_{32} = \frac{1}{2}$.

If ρ is (-1) -stretchable or 2-producible, $\Gamma_{2\text{-prod}}^{\max}$ is a set of partitions having the type $\{2, 2, 1\}$. We select $P_2 = \{\rho_{1,16}\}$. By the codes in [44], one of the criteria is

$$|\rho_{1,16}| \leq \text{Tr}[W_{2\text{-prod}} \cdot \rho], \quad (27)$$

where $W_{2\text{-prod}} = \text{diag}\{a_1, \dots\}$ is the diagonal matrix with $a_4 = a_6 = a_7 = a_{10} = a_{11} = a_{13} = \frac{1}{2}$.

If ρ is 0-stretchable or 1-stretchable or 3-producible or 3-partitionable, one of the criteria is

$$\sum_{\rho_{m,n} \in P} |\rho_{m,n}| \leq \text{Tr}[W_{3\text{-part}} \cdot \rho], \quad (28)$$

where $W_{3\text{-part}} = \text{diag}\{a_1, \dots\}$ is the diagonal matrix with $a_4 = a_{13} = a_{17} = a_{32} = 1$, and $a_1 = a_2 = a_3 = a_5 = a_6 = a_7 = a_8 = a_9 = a_{10} = a_{11} = a_{12} = a_{14} = a_{15} = a_{16} = a_{18} = a_{19} = a_{20} = a_{21} = a_{22} = a_{23} = a_{24} = a_{25} = a_{26} = a_{27} = a_{28} = a_{29} = a_{30} = a_{31} = \frac{1}{2}$.

If ρ is 2-stretchable or 2-partitionable or 4-producible, one of the criteria is

$$\sum_{\rho_{m,n} \in P} |\rho_{m,n}| \leq \text{Tr}[W_{4\text{-prod}} \cdot \rho], \quad (29)$$

where $W_{4\text{-prod}} = \text{diag}\{a_1, \dots\}$ is the diagonal matrix with $a_2 = a_3 = a_4 = a_5 = a_8 = a_9 = a_{12} = a_{13} = a_{14} = a_{15} = a_{17} = a_{18} = a_{19} = a_{21} = a_{24} = a_{25} = a_{28} = a_{30} = a_{31} = a_{32} = 1$, and $a_1 = a_6 = a_7 = a_{10} = a_{11} = a_{16} = a_{20} = a_{22} = a_{23} = a_{26} = a_{27} = a_{29} = \frac{1}{2}$.

The observables W_P and $W_{k\text{-prod}}$, $W_{k\text{-part}}$ and $W_{k\text{-str}}$ are expressed as follows

$$\begin{aligned} W_P &= Z_1^+ \otimes \left(\bigotimes_{i=2}^5 H_i^+ \right) + Z_2^+ \otimes Z_3^+ \otimes H_1^+ \otimes H_4^+ \otimes H_5^+ \\ &+ Z_4^+ \otimes Z_5^+ \otimes H_1^+ \otimes H_2^+ \otimes H_3^+ + Z_2^- \otimes Z_3^- \otimes H_1^+ \\ &\otimes H_4^- \otimes H_5^- + Z_4^- \otimes Z_5^- \otimes H_1^+ \otimes H_2^- \otimes H_3^- \\ &+ Z_1^- \otimes H_2^+ \otimes H_3^+ \otimes H_4^- \otimes H_5^- \\ W_{P_2} &= Z_1^+ \otimes \left(\bigotimes_{i=2}^5 H_i^+ \right) \\ W_{4\text{-part}} &= \frac{\mathbb{I}_{32} - \Delta_1}{2} \\ W_{2\text{-prod}} &= \frac{1}{2} Z_1^+ \otimes \sum_{2 \leq i < j \leq 5} [Z_i^+ \otimes Z_j^+ \otimes \left(\bigotimes_{\substack{2 \leq k \leq 5, \\ k \neq i, j}} Z_k^- \right)] \\ W_{3\text{-part}} &= \frac{\mathbb{I}}{2} + \frac{\Delta_2}{2} \\ W_{4\text{-prod}} &= \mathbb{I} - \frac{\Delta_1}{2} \end{aligned} \quad (30)$$

with

$$\begin{aligned} \Delta_1 &= (Z_1^- + Z_1^+) \otimes \left[\sum_{\substack{2 \leq i \leq 3, \\ 4 \leq j \leq 5}} Z_i^+ \otimes Z_j^+ \otimes \left(\bigotimes_{\substack{2 \leq k \leq 5, \\ k \neq i, j}} Z_k^- \right) \right] \\ &+ \bigotimes_{i=1}^5 Z_i^- + Z_1^- \otimes \left(\bigotimes_{i=2}^5 Z_i^+ \right) + Z_1^+ \otimes (Z_2^- \otimes Z_3^- \otimes Z_4^+ \\ &\otimes Z_5^+ + Z_2^+ \otimes Z_3^+ \otimes Z_4^- \otimes Z_5^-) \\ \Delta_2 &= Z_1^- \otimes (Z_2^- \otimes Z_3^- \otimes Z_4^+ \otimes Z_5^+ + Z_2^+ \otimes Z_3^+ \otimes Z_4^- \\ &\otimes Z_5^- + Z_1^+ \otimes \left(\bigotimes_{i=2}^5 Z_i^- + \bigotimes_{i=2}^5 Z_i^+ \right) \end{aligned} \quad (31)$$

The details of Example 4.

Unless otherwise specified, we select $P = \{\rho_{1,64}\}$.

Different from other examples, we fix the right-hand side of the inequality and seek a larger left-hand side, the details are listed as follows.

If ρ is 1-producible, one of the criteria is

$$|\rho_{1,64}| \leq \text{Tr}[W_{1\text{-prod}} \cdot \rho], \quad (32)$$

where $W_{1\text{-prod}} = \text{diag}\{a_1, \dots, a_{64}\}$ is the diagonal matrix with $a_2 = a_{63} = \frac{1}{2}$.

If ρ is 5-partitionable or (-3) -stretchable, $\Gamma_{5\text{-part}}^{\max}$ is a set of partitions of type $\{2, 1, 1, 1, 1\}$. Consider six inequalities derived from Proposition 1, corresponding to the parts $\{1\}$, $\{2\}$, $\{3\}$, $\{4\}$, $\{5\}$, and $\{6\}$, respectively. Given each partition in the current set includes four parts, summing the corresponding four inequalities yields the inequality for that partition. Thus the criterion is

$$4|\rho_{1,64}| \leq \text{Tr}[W_{5\text{-part}} \cdot \rho], \quad (33)$$

where $W_{5\text{-part}} = \text{diag}\{a_1, \dots\}$ is the diagonal matrix with $a_2 = a_3 = a_5 = a_9 = a_{17} = a_{32} = a_{33} = a_{48} = a_{56} = a_{60} = a_{62} = a_{63} = \frac{1}{2}$.

If ρ is 4-partitionable, $\Gamma_{4\text{-part}}^{\max}$ is a set of partitions of type $\{2, 2, 1, 1\}$ and $\{3, 1, 1, 1\}$. Given each partition in the current set includes two parts, with each part containing one subsystem, the criterion is

$$2|\rho_{1,64}| \leq \text{Tr}[W_{4\text{-part}} \cdot \rho], \quad (34)$$

where $W_{4\text{-part}} = W_{5\text{-part}}$.

If ρ is (-2) -stretchable, $\Gamma_{(-2)\text{-str}}^{\max}$ is a set of partitions of type $\{2, 2, 1, 1\}$. Therefore, the criterion is given by the inequality (34).

If ρ is (-1) -stretchable, $\Gamma_{(-1)\text{-str}}^{\max}$ is a set of partitions of types $\{2, 2, 2\}$ and $\{3, 1, 1, 1\}$. We consider 15 inequalities derived from Proposition 1, each corresponding to

a part that includes two subsystems. For each partition in the set of partitions of type $\{2, 2, 2\}$, which includes three parts each containing two subsystems, the inequality for that partition is obtained by summing the corresponding three inequalities. Similarly, we consider six inequalities, each corresponding to a part that contains one subsystem. For each partition in the set of partitions of type $\{3, 1, 1, 1\}$, which includes three parts each containing one subsystem, the inequality for that partition is obtained by summing the corresponding three inequalities. Therefore, the criterion is of the form,

$$3|\rho_{1,64}| \leq \text{Tr}[W_{(-1)\text{-str}} \cdot \rho], \quad (35)$$

where $W_{(-1)\text{-str}} = \text{diag}\{a_1, \dots\}$ is the diagonal matrix with $a_2 = a_3 = a_4 = a_5 = a_6 = a_7 = a_9 = a_{10} = a_{11} = a_{13} = a_{16} = a_{17} = a_{18} = a_{19} = a_{21} = a_{24} = a_{25} = a_{28} = a_{30} = a_{31} = a_{32} = a_{33} = a_{34} = a_{35} = a_{37} = a_{40} = a_{41} = a_{44} = a_{46} = a_{47} = a_{48} = a_{49} = a_{52} = a_{54} = a_{55} = a_{56} = a_{58} = a_{60} = a_{59} = a_{61} = a_{62} = a_{63} = \frac{1}{2}$.

If ρ is 3-partitionable, $\Gamma_{3\text{-part}}^{\max}$ is a set of partitions of types $\{2, 2, 2\}$, $\{3, 2, 1\}$ and $\{4, 1, 1\}$. For each partition in the set of partitions of type $\{2, 2, 2\}$, we also consider 15 inequalities as before. For each partition in the set of partitions of type $\{4, 1, 1\}$, we further consider six inequalities, each corresponding to a part that, as in the previous cases, contains one subsystem. Employing the codes in [44], for each partition in the set of partitions of type $\{3, 2, 1\}$, we sum the six inequalities twice. Therefore, we have

$$3|\rho_{1,64}| \leq \text{Tr}[W_{3\text{-part}} \cdot \rho], \quad (36)$$

where $W_{3\text{-part}} = \text{diag}\{a_1, \dots\}$ is the diagonal matrix with $a_2 = a_3 = a_5 = a_9 = a_{17} = a_{32} = a_{33} = a_{48} = a_{56} = a_{60} = a_{62} = a_{63} = 1$ and $a_4 = a_6 = a_7 = a_{10} = a_{11} = a_{13} = a_{16} = a_{18} = a_{19} = a_{21} = a_{24} = a_{25} = a_{28} = a_{30} = a_{31} = a_{34} = a_{35} = a_{37} = a_{40} = a_{41} = a_{44} = a_{46} = a_{47} = a_{49} = a_{52} = a_{54} = a_{55} = a_{58} = a_{59} = a_{61} = \frac{1}{2}$.

If ρ is 0-stretchable, $\Gamma_{0\text{-str}}^{\max}$ is a set of partitions of types $\{2, 2, 2\}$ and $\{3, 2, 1\}$. The criteria is given by the inequality (36).

The inequalities (33, 34, 35, 36) are all derived using the approach of fixing the right-hand side of the inequality and seeking a larger left-hand side.

If ρ is 2-producible, $\Gamma_{2\text{-prod}}^{\max}$ is a set of partitions of type $\{2, 2, 2\}$. By the codes in [44], one of the criteria is

$$|\rho_{1,64}| \leq \text{Tr}[W_{2\text{-prod}} \cdot \rho], \quad (37)$$

where $W_{2\text{-prod}} = \text{diag}\{a_1, \dots\}$ is the diagonal matrix with $a_4 = a_7 = a_{11} = a_{19} = a_{30} = a_{35} = a_{46} = a_{54} = a_{58} = a_{61} = \frac{1}{2}$.

If ρ is 3-producible, $\Gamma_{3\text{-prod}}^{\max}$ is a set of partitions of types $\{2, 2, 2\}$ and $\{3, 3\}$. By the codes in [44], one of the criteria is

$$|\rho_{1,64}| \leq \text{Tr}[W_{3\text{-prod}} \cdot \rho], \quad (38)$$

where $W_{3\text{-prod}} = \text{diag}\{a_1, \dots\}$ is the diagonal matrix with $a_4 = a_7 = a_8 = a_{11} = a_{12} = a_{14} = a_{15} = a_{19} = a_{20} = a_{22} = a_{23} = a_{26} = a_{27} = a_{29} = a_{30} = a_{35} = a_{36} = a_{38} = a_{39} = a_{42} = a_{43} = a_{45} = a_{46} = a_{50} = a_{51} = a_{53} = a_{54} = a_{57} = a_{58} = a_{61} = \frac{1}{2}$

If ρ is 1-stretchable, $\Gamma_{1\text{-str}}^{\max}$ is a set of partitions of types $\{2, 2, 2\}$, $\{3, 3\}$ and $\{4, 1, 1\}$. By the codes in [44], one of the criteria is

$$|\rho_{1,64}| \leq \text{Tr}[W_{1\text{-str}} \cdot \rho], \quad (39)$$

where $W_{1\text{-str}} = \text{diag}\{a_1, \dots\}$ is the diagonal matrix with $a_2 = a_3 = a_4 = a_5 = a_7 = a_8 = a_9 = a_{11} = a_{12} = a_{14} = a_{15} = a_{17} = a_{19} = a_{20} = a_{22} = a_{23} = a_{26} = a_{27} = a_{29} = a_{30} = a_{35} = a_{36} = a_{38} = a_{39} = a_{42} = a_{43} = a_{45} = a_{46} = a_{48} = a_{50} = a_{51} = a_{53} = a_{54} = a_{56} = a_{57} = a_{58} = a_{60} = a_{61} = a_{62} = a_{63} = \frac{1}{2}$.

If ρ is 4-producible or 2-stretchable, $\Gamma_{4\text{-prod}}^{\max}$ is a set of partitions of types $\{4, 2\}$ and $\{3, 3\}$, and the criterion is given by

$$|\rho_{1,64}| \leq \text{Tr}[W_{4\text{-prod}} \cdot \rho], \quad (40)$$

where $W_{4\text{-prod}}^P = \text{diag}\{a_1, \dots\}$ is the diagonal matrix with $a_4 = a_6 = a_7 = a_8 = a_{10} = a_{11} = a_{12} = a_{13} = a_{14} = a_{15} = a_{16} = a_{18} = a_{19} = a_{20} = a_{21} = a_{22} = a_{23} = a_{24} = a_{25} = a_{26} = a_{27} = a_{28} = a_{29} = a_{30} = a_{31} = a_{34} = a_{35} = a_{36} = a_{37} = a_{38} = a_{39} = a_{40} = a_{41} = a_{42} = a_{43} = a_{44} = a_{45} = a_{46} = a_{47} = a_{49} = a_{50} = a_{51} = a_{52} = a_{53} = a_{54} = a_{55} = a_{57} = a_{58} = a_{59} = a_{61} = \frac{1}{2}$.

If ρ is 5-producible or 3-stretchable, $\Gamma_{4\text{-prod}}^{\max}$ is a set of partitions of types $\{5, 1\}$, $\{4, 2\}$ and $\{3, 3\}$, and the criterion is

$$|\rho_{1,64}| \leq \text{Tr}[W_{5\text{-prod}} \cdot \rho], \quad (41)$$

where $W_{5\text{-prod}} = \text{diag}\{a_1, \dots\}$ is the diagonal matrix with $a_2 = a_3 = a_4 = a_5 = a_6 = a_7 = a_8 = a_9 = a_{10} = a_{11} = a_{12} = a_{13} = a_{14} = a_{15} = a_{16} = a_{17} = a_{18} = a_{19} = a_{20} = a_{21} = a_{22} = a_{23} = a_{24} = a_{25} = a_{26} = a_{27} = a_{28} = a_{29} = a_{30} = a_{31} = a_{32} = a_{33} = a_{34} = a_{35} = a_{36} = a_{37} = a_{38} = a_{39} = a_{40} = a_{41} = a_{42} = a_{43} = a_{44} = a_{45} = a_{46} = a_{47} = a_{48} = a_{49} = a_{50} = a_{51} = a_{52} = a_{53} = a_{54} = a_{55} = a_{56} = a_{57} = a_{58} = a_{59} = a_{60} = a_{61} = a_{62} = a_{63} = \frac{1}{2}$.

The observables W_P and $W_{k\text{-prod}}$, $W_{k\text{-part}}$ and $W_{k\text{-str}}$

are expressed as follows

$$\begin{aligned}
W_P &= \bigotimes_{i=1}^n H_i^+ + \bigotimes_{i=1}^n H_i^- \\
W_{1\text{-prod}} &= \frac{1}{2}(Z_1^+ Z_2^+ Z_3^+ Z_4^+ Z_5^+ Z_6^- + Z_1^- Z_2^- Z_3^- Z_4^- Z_5^- Z_6^+) \\
W_{2\text{-prod}} &= \frac{1}{2}(\Delta_1 + X\Delta_1 X) \\
W_{3\text{-prod}} &= \frac{1}{2}(\Delta_1 + X\Delta_1 X + \Delta_2 + X\Delta_2 X + \Delta_3 + X\Delta_3 X) \\
W_{4\text{-prod}} &= \frac{\mathbb{I}_{64}}{2} - \frac{1}{2} \bigotimes_{k=1}^6 Z_k^+ - \frac{1}{2} \bigotimes_{k=1}^6 Z_k^- - \\
&\quad \frac{1}{2} \sum_{k=1}^6 Z_k^- \otimes \left(\bigotimes_{j \neq k} Z_j^+ \right) - \frac{1}{2} \sum_{k=1}^6 Z_k^+ \otimes \left(\bigotimes_{j \neq k} Z_j^- \right) \\
W_{5\text{-prod}} &= \frac{\mathbb{I}_{64}}{2} - \frac{1}{2} \bigotimes_{k=1}^6 Z_k^+ - \frac{1}{2} \bigotimes_{k=1}^6 Z_k^- \\
W_{1\text{-str}} &= \frac{\mathbb{I}_{64}}{2} - \frac{1}{2}(\Delta_4 + X\Delta_4 X + \bigotimes_{i=2}^6 Z_i^+ + \bigotimes_{i=2}^6 Z_i^-) \\
W_{-1\text{-str}} &= \frac{\mathbb{I}_{64}}{2} - \frac{1}{2}(\Delta_2 + X\Delta_2 X + \Delta_3 + X\Delta_3 X + \\
&\quad \bigotimes_{i=1}^6 Z_i^+ + \bigotimes_{i=1}^6 Z_i^-) \\
W_{3\text{-part}} &= \frac{\mathbb{I}_{64}}{2} + \frac{1}{2}(\Delta_5 + X\Delta_5 X - \Delta_2 - X\Delta_2 X - \Delta_3 \\
&\quad - X\Delta_3 X - \bigotimes_{i=1}^6 Z_i^+ - \bigotimes_{i=1}^6 Z_i^-)
\end{aligned} \tag{42}$$

$$\begin{aligned}
W_{4\text{-part}} &= W_{5\text{-part}}^P = \sum_{k=1}^6 Z_k^- \otimes \left(\bigotimes_{j=1, j \neq k}^6 Z_j^+ \right) \\
&\quad + \sum_{k=1}^6 Z_k^+ \otimes \left(\bigotimes_{j=1, j \neq k}^6 Z_j^- \right)
\end{aligned} \tag{43}$$

with

$$\begin{aligned}
X &= \bigotimes_{i=1}^6 \sigma_x^{(i)} \\
\Delta_1 &= Z_1^+ Z_2^+ (Z_3^+ Z_4^+ Z_5^- Z_6^- + Z_3^+ Z_4^- Z_5^- Z_6^+ + Z_3^- Z_4^+ Z_5^- Z_6^+) \\
&\quad + (Z_1^+ Z_2^- + Z_1^- Z_2^+) Z_3^+ Z_4^+ Z_5^- Z_6^- \\
\Delta_2 &= Z_1^+ Z_2^+ (Z_3^+ Z_4^+ Z_5^- Z_6^- + Z_3^+ Z_4^- Z_5^- Z_6^+ + Z_3^- Z_4^+ Z_5^- Z_6^+ \\
&\quad + Z_3^- Z_4^+ Z_5^+ Z_6^+) \\
\Delta_3 &= Z_1^+ Z_2^- (Z_3^+ Z_4^+ Z_5^- Z_6^- + Z_3^+ Z_4^- Z_5^- Z_6^+ + Z_3^- Z_4^+ Z_5^- Z_6^+ \\
&\quad + Z_3^- Z_4^- Z_5^+ Z_6^+ + Z_3^- Z_4^+ Z_5^- Z_6^- + Z_3^+ Z_4^- Z_5^+ Z_6^-) \\
\Delta_4 &= (Z_1^+ Z_2^- + Z_1^- Z_2^+) (Z_3^+ Z_4^+ Z_5^- Z_6^- + Z_3^+ Z_4^- Z_5^+ Z_6^- \\
&\quad + Z_3^- Z_4^+ Z_5^+ Z_6^+) + Z_1^+ Z_2^+ (Z_3^+ Z_4^- Z_5^- Z_6^- \\
&\quad + Z_3^- Z_4^+ Z_5^+ Z_6^- + Z_3^- Z_4^- Z_5^+ Z_6^+ Z_3^- Z_4^- Z_5^- Z_6^-) \\
\Delta_5 &= \sum_{i=1}^6 Z_i^- \otimes \left(\bigotimes_{j=1, j \neq i}^6 Z_j^+ \right)
\end{aligned} \tag{44}$$

and $\sigma_x^{(i)}$ being the pauli matrice in the i -th subsystem.

-
- [1] O. Gühne and G. Tóth, Entanglement detection, Phys. Rep. **474**, 1 (2009).
- [2] A. S. Sørensen and K. Mølmer, Entanglement and extreme spin squeezing, Phys. Rev. Lett. **86**, 4431 (2001).
- [3] O. Gühne, G. Tóth, and H. J. Briegel, Multipartite entanglement in spin chains, New J. Phys. **7**, 229 (2005).
- [4] S. Szalay, k -stretchability of entanglement, and the duality of k -separability and k -producibility, Quantum **3**, 204 (2019).
- [5] O. Gühne and G. Tóth, Energy and multipartite entanglement in multidimensional and frustrated spin models, Phys. Rev. A **73**, 052319 (2006).
- [6] G. Tóth, Multipartite entanglement and high-precision metrology, Phys. Rev. A **85**, 022322 (2012).
- [7] Z. Ren, W. Li, A. Smerzi, and M. Gessner, Metrological detection of multipartite entanglement from young diagrams, Phys. Rev. Lett. **126**, 080502 (2021).
- [8] B. Jungnitsch, T. Moroder, and O. Gühne, Taming multiparticle entanglement, Phys. Rev. Lett. **106**, 190502 (2011).
- [9] M. Huber, F. Mintert, A. Gabriel, and B. C. Hiesmayr, Detection of high-dimensional genuine multipartite entanglement of mixed states, Phys. Rev. Lett. **104**, 210501 (2010).
- [10] J. Bae, D. Chruściński, and B. C. Hiesmayr, Mirrored entanglement witnesses, npj Quantum Inf **6**, 15 (2020).
- [11] B. Jungnitsch, T. Moroder, and O. Gühne, Entanglement witnesses for graph states: General theory and examples, Phys. Rev. A **84**, 032310 (2011).
- [12] F. Huber, O. Gühne, and J. Siewert, Absolutely maximally entangled states of seven qubits do not exist, Phys. Rev. Lett. **118**, 200502 (2017).
- [13] Y. Hong, S. Luo, and H. Song, Detecting k -nonseparability via quantum fisher information, Phys. Rev. A **91**, 042313 (2015).
- [14] X.-Y. Chen, L.-Z. Jiang, and Z.-A. Xu, Necessary and sufficient criterion for k -separability of n -qubit noisy ghz states, Int. J. Quantum Inform. **16**, 1850037 (2018).
- [15] Y. Hong and S. Luo, Detecting k -nonseparability via local uncertainty relations, Phys. Rev. A **93**, 042310 (2016).
- [16] T. Gao, F. Yan, and S. J. van Enk, Permutationally invariant part of a density matrix and nonseparability of n -qubit states, Phys. Rev. Lett. **112**, 180501 (2014).

- [17] Y. Hong, T. Gao, and F. Yan, Detection of k-partite entanglement and k-nonnseparability of multipartite quantum states, *Phys. Lett. A* **401**, 127347 (2021).
- [18] G. Vitagliano, P. Hyllus, I. n. L. Egusquiza, and G. Tóth, Spin squeezing inequalities for arbitrary spin, *Phys. Rev. Lett.* **107**, 240502 (2011).
- [19] Z. Chen, Wigner-yanase skew information as tests for quantum entanglement, *Phys. Rev. A* **71**, 052302 (2005).
- [20] P. Hyllus, W. Laskowski, R. Krischek, C. Schwemmer, W. Wieczorek, H. Weinfurter, L. Pezzè, and A. Smerzi, Fisher information and multipartite entanglement, *Phys. Rev. A* **85**, 022321 (2012).
- [21] M. Gessner, L. Pezzè, and A. Smerzi, Efficient entanglement criteria for discrete, continuous, and hybrid variables, *Phys. Rev. A* **94**, 020101 (2016).
- [22] C. Chen, C. Ren, H. Lin, and H. Lu, Entanglement structure detection via machine learning, *Quantum Sci. Technol.* **6**, 035017 (2021).
- [23] Y. Zhou, Q. Zhao, X. Yuan, and X. Ma, Detecting multipartite entanglement structure with minimal resources, *npj Quantum Inf* **5**, 83 (2019).
- [24] J.-Y. Chen, Z. Ji, N. Yu, and B. Zeng, Entanglement depth for symmetric states, *Phys. Rev. A* **94**, 042333 (2016).
- [25] J.-D. Bancal, N. Gisin, Y.-C. Liang, and S. Pironio, Device-independent witnesses of genuine multipartite entanglement, *Phys. Rev. Lett.* **106**, 250404 (2011).
- [26] D. Collins, N. Gisin, S. Popescu, D. Roberts, and V. Scarani, Bell-type inequalities to detect true n -body nonseparability, *Phys. Rev. Lett.* **88**, 170405 (2002).
- [27] A. Aloy, J. Tura, F. Baccari, A. Acín, M. Lewenstein, and R. Augusiak, Device-independent witnesses of entanglement depth from two-body correlators, *Phys. Rev. Lett.* **123**, 100507 (2019).
- [28] P.-S. Lin, J.-C. Hung, C.-H. Chen, and Y.-C. Liang, Exploring bell inequalities for the device-independent certification of multipartite entanglement depth, *Phys. Rev. A* **99**, 062338 (2019).
- [29] Y.-C. Liang, D. Rosset, J.-D. Bancal, G. Pütz, T. J. Barnea, and N. Gisin, Family of bell-like inequalities as device-independent witnesses for entanglement depth, *Phys. Rev. Lett.* **114**, 190401 (2015).
- [30] J. Tura, A. Aloy, F. Baccari, A. Acín, M. Lewenstein, and R. Augusiak, Optimization of device-independent witnesses of entanglement depth from two-body correlators, *Phys. Rev. A* **100**, 032307 (2019).
- [31] M. Lewenstein, G. Müller-Rigat, J. Tura, and A. Sanpera, Linear maps as sufficient criteria for entanglement depth and compatibility in many-body systems, *Open Syst. Inf. Dyn.* **29**, 2250011 (2022).
- [32] C. Gross, T. Zibold, E. Nicklas, J. Estève, and M. K. Oberthaler, Nonlinear atom interferometer surpasses classical precision limit, *Nature* **464**, 1165 (2010).
- [33] B. Lücke, J. Peise, G. Vitagliano, J. Arlt, L. Santos, G. Tóth, and C. Klempt, Detecting multipartite entanglement of dicke states, *Phys. Rev. Lett.* **112**, 155304 (2014).
- [34] O. Hosten, N. J. Engelsen, R. Krishnakumar, and M. A. Kasevich, Measurement noise 100 times lower than the quantum-projection limit using entangled atoms, *Nature* **529**, 505 (2016).
- [35] R. McConnell, H. Zhang, J. Hu, S. Čuk, and V. Vuletić, Entanglement with negative wigner function of almost 3,000 atoms heralded by one photon, *Nature* **519**, 439 (2015).
- [36] F. Haas, J. Volz, R. Gehr, J. Reichel, and J. Estève, Entangled states of more than 40 atoms in an optical fiber cavity, *Science* **344**, 180 (2014).
- [37] Y.-Q. Zou, L.-N. Wu, Q. Liu, X.-Y. Luo, S.-F. Guo, J.-H. Cao, M. K. Tey, and L. You, Beating the classical precision limit with spin-1 dicke states of more than 10,000 atoms, *Proc. Natl. Acad. Sci. U.S.A.* **115**, 6381 (2018).
- [38] H. Lu, Q. Zhao, Z.-D. Li, X.-F. Yin, X. Yuan, J.-C. Hung, L.-K. Chen, L. Li, N.-L. Liu, C.-Z. Peng, Y.-C. Liang, X. Ma, Y.-A. Chen, and J.-W. Pan, Entanglement structure: Entanglement partitioning in multipartite systems and its experimental detection using optimizable witnesses, *Phys. Rev. X* **8**, 021072 (2018).
- [39] Y. Tian, L. Che, X. Long, C. Ren, and D. Lu, Machine learning experimental multipartite entanglement structure, *Adv Quantum Technol.* **5**, 2200025 (2022).
- [40] G. Tóth, Stretching the limits of multipartite entanglement, *Quantum Views* **4**, 30 (2020).
- [41] T.-A. Ohst, X.-D. Yu, O. Gühne, and H. C. Nguyen, Certifying quantum separability with adaptive polytopes, *SciPost Phys.* **16**, 063 (2024).
- [42] B. Grünbaum, V. Klee, M. A. Perles, and G. C. Shephard, *Convex polytopes*, Vol. 16 (Springer, 1967).
- [43] B. Legat, Polyhedral computation, in *JuliaCon* (2023).
- [44] Quantum entanglement structure detection, github repository: https://github.com/JMU-Quantum-Group/Quantum_entanglement_structure_detection.
- [45] J. Shang and O. Gühne, Convex optimization over classes of multipartite entanglement, *Phys. Rev. Lett.* **120**, 050506 (2018).
- [46] F. Bohnet-Waldraff, D. Braun, and O. Giraud, Entanglement and the truncated moment problem, *Phys. Rev. A* **96**, 032312 (2017).
- [47] G. Sagnol and M. Stahlberg, PICOS: A Python interface to conic optimization solvers, *Journal of Open Source Software* **7**, 3915 (2022).
- [48] D. E. Knuth, Dancing links (2000), arXiv:cs/0011047 [cs.DS].